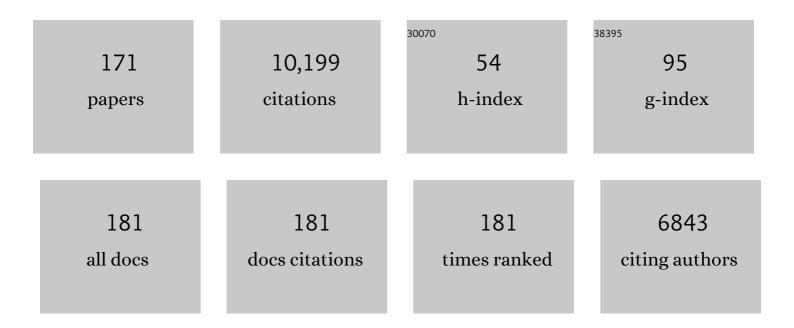
List of Publications by Year in descending order

Source: https://exaly.com/author-pdf/2491436/publications.pdf Version: 2024-02-01



#	Article	IF	CITATIONS
1	Personalized Risk Model and Leveraging of Magnetic Resonance Imaging–Based Structural Phenotypes and Clinical Factors to Predict Incidence of Radiographic Osteoarthritis. Arthritis Care and Research, 2023, 75, 501-508.	3.4	5
2	Changes in Hip Capsule Morphology after Arthroscopic Treatment for Femoroacetabular Impingement Syndrome with Periportal Capsulotomy are Correlated With Improvements in Patient-Reported Outcomes. Arthroscopy - Journal of Arthroscopic and Related Surgery, 2022, 38, 394-403.	2.7	12
3	Magnetizationâ€prepared spoiled gradientâ€echo snapshot imaging for efficient measurement of R ₂ â€R _{1Ï} in knee cartilage. Magnetic Resonance in Medicine, 2022, 87, 733-745.	3.0	5
4	Al MSK clinical applications: cartilage and osteoarthritis. Skeletal Radiology, 2022, 51, 331-343.	2.0	12
5	Studying osteoarthritis with artificial intelligence applied to magnetic resonance imaging. Nature Reviews Rheumatology, 2022, 18, 112-121.	8.0	23
6	Institutionâ€wide shape analysis of 3D spinal curvature and global alignment parameters. Journal of Orthopaedic Research, 2022, 40, 1896-1908.	2.3	3
7	Subjectâ€specific biomechanical analysis to estimate locations susceptible to osteoarthritis—Finite element modeling and MRI followâ€up of ACL reconstructed patients. Journal of Orthopaedic Research, 2022, 40, 1744-1755.	2.3	8
8	Surface spherical encoding and contrastive learning for virtual bone shape aging. Medical Image Analysis, 2022, 77, 102388.	11.6	3
9	FDA/Arthritis Foundation osteoarthritis drug development workshop recap: Assessment of long-term benefit. Seminars in Arthritis and Rheumatism, 2022, 56, 152070.	3.4	12
10	Multiparametric MRI characterization of knee articular cartilage and subchondral bone shape in collegiate basketball players. Journal of Orthopaedic Research, 2021, 39, 1512-1522.	2.3	8
11	Patients with Symptomatic Hip Osteoarthritis Have Altered Kinematics during Stair Ambulation. PM and R, 2021, 13, 128-136.	1.6	2
12	Correlation of hip capsule morphology with patient symptoms from femoroacetabular impingement. Journal of Orthopaedic Research, 2021, 39, 590-596.	2.3	8
13	T ₂ analysis of the entire osteoarthritis initiative dataset. Journal of Orthopaedic Research, 2021, 39, 74-85.	2.3	23
14	Multivariate functional principal component analysis identifies waveform features of gait biomechanics related to earlyâ€ŧoâ€moderate hip osteoarthritis. Journal of Orthopaedic Research, 2021, 39, 1722-1731.	2.3	2
15	Longitudinal analysis of the contribution of 3D patella and trochlear bone shape on patellofemoral joint osteoarthritic features. Journal of Orthopaedic Research, 2021, 39, 506-515.	2.3	12
16	Towards understanding mechanistic subgroups of osteoarthritis: 8â€year cartilage thickness trajectory analysis. Journal of Orthopaedic Research, 2021, 39, 1305-1317.	2.3	16
17	Automatic hip abductor muscle fat fraction estimation and association with early OA cartilage degeneration biomarkers. Journal of Orthopaedic Research, 2021, 39, 2376-2387.	2.3	3
18	Effects of the Competitive Season and Off‣eason on Knee Articular Cartilage in Collegiate Basketball Players Using Quantitative MRI: A Multicenter Study. Journal of Magnetic Resonance Imaging, 2021, 54, 840-851.	3.4	9

#	Article	IF	CITATIONS
19	Weight Cycling and Knee Joint Degeneration in Individuals with Overweight or Obesity: Four‥ear Magnetic Resonance Imaging Data from the Osteoarthritis Initiative. Obesity, 2021, 29, 909-918.	3.0	4
20	Automatic Deep Learning–assisted Detection and Grading of Abnormalities in Knee MRI Studies. Radiology: Artificial Intelligence, 2021, 3, e200165.	5.8	46
21	The International Workshop on Osteoarthritis Imaging Knee MRI Segmentation Challenge: A Multi-Institute Evaluation and Analysis Framework on a Standardized Dataset. Radiology: Artificial Intelligence, 2021, 3, e200078.	5.8	46
22	Deep learning for large scale MRI-based morphological phenotyping of osteoarthritis. Scientific Reports, 2021, 11, 10915.	3.3	21
23	Longitudinal Changes of Patellar Alignment Before and After Anterior Cruciate Ligament Reconstruction With Hamstring Autograft. American Journal of Sports Medicine, 2021, 49, 2908-2915.	4.2	4
24	Federated learning for predicting clinical outcomes in patients with COVID-19. Nature Medicine, 2021, 27, 1735-1743.	30.7	300
25	Uncovering associations between data-driven learned qMRI biomarkers and chronic pain. Scientific Reports, 2021, 11, 21989.	3.3	10
26	Augmenting Osteoporosis Imaging with Machine Learning. Current Osteoporosis Reports, 2021, 19, 699-709.	3.6	1
27	Cam morphology is associated with MRI-defined cartilage defects and labral tears: a case–control study of 237 young adult football players with and without hip and groin pain. BMJ Open Sport and Exercise Medicine, 2021, 7, e001199.	2.9	11
28	Postoperative MRI Findings and Associated Pain Changes After Arthroscopic Surgery for Femoroacetabular Impingement. American Journal of Roentgenology, 2020, 214, 177-184.	2.2	11
29	Extracting Voxelâ€Based Cartilage Relaxometry Features in Hip Osteoarthritis Subjects Using Principal Component Analysis. Journal of Magnetic Resonance Imaging, 2020, 51, 1708-1719.	3.4	2
30	Quantitative imaging of anterior cruciate ligament (ACL) graft demonstrates longitudinal compositional changes and relationships with clinical outcomes at 2 years after ACL reconstruction. Journal of Orthopaedic Research, 2020, 38, 1289-1295.	2.3	27
31	Rapid Knee MRI Acquisition and Analysis Techniques for Imaging Osteoarthritis. Journal of Magnetic Resonance Imaging, 2020, 52, 1321-1339.	3.4	38
32	Short term outcomes of hip arthroscopy on hip joint mechanics and cartilage health in patients with femoroacetabular impingement syndrome. Clinical Biomechanics, 2020, 71, 214-220.	1.2	14
33	Patellar Malalignment Is Associated With Patellofemoral Lesions and Cartilage Relaxation Times After Hamstring Autograft Anterior Cruciate Ligament Reconstruction. American Journal of Sports Medicine, 2020, 48, 2242-2251.	4.2	10
34	Automatic Hip Fracture Identification and Functional Subclassification with Deep Learning. Radiology: Artificial Intelligence, 2020, 2, e190023.	5.8	72
35	Deep Learning for Hierarchical Severity Staging of Anterior Cruciate Ligament Injuries from MRI. Radiology: Artificial Intelligence, 2020, 2, e190207.	5.8	32
36	Principal Component Analysis of Simultaneous PETâ€MRI Reveals Patterns of Bone–Cartilage Interactions in Osteoarthritis. Journal of Magnetic Resonance Imaging, 2020, 52, 1462-1474.	3.4	22

#	Article	IF	CITATIONS
37	Lumbar intervertebral disc characterization through quantitative MRI analysis: An automatic voxelâ€based relaxometry approach. Magnetic Resonance in Medicine, 2020, 84, 1376-1390.	3.0	16
38	Learning osteoarthritis imaging biomarkers from bone surface spherical encoding. Magnetic Resonance in Medicine, 2020, 84, 2190-2203.	3.0	34
39	Computerâ€Aided Detection <scp>Al</scp> Reduces <scp>Interreader</scp> Variability in Grading Hip Abnormalities With <scp>MRI</scp> . Journal of Magnetic Resonance Imaging, 2020, 52, 1163-1172.	3.4	14
40	Deep Learning Predicts Total Knee Replacement from Magnetic Resonance Images. Scientific Reports, 2020, 10, 6371.	3.3	73
41	In Memoriam – Harry K. Genant, MD. Journal of Bone and Mineral Research, 2020, 37, 819-823.	2.8	0
42	Validation of scoring hip osteoarthritis with MRI (SHOMRI) scores using hip arthroscopy as a standard of reference. European Radiology, 2019, 29, 578-587.	4.5	21
43	Association Between Gait Kinetics and Symptomatic Progression in Persons With Patellofemoral With/Without Concurrent Tibiofemoral Osteoarthritis. Journal of Orthopaedic Research, 2019, 37, 2593-2600.	2.3	7
44	Variation in the Thickness of Knee Cartilage. The Use of a Novel Machine Learning Algorithm for Cartilage Segmentation of Magnetic Resonance Images. Journal of Arthroplasty, 2019, 34, 2210-2215.	3.1	32
45	Quantitative [¹⁸ F]-Naf-PET-MRI Analysis for the Evaluation of Dynamic Bone Turnover in a Patient with Facetogenic Low Back Pain. Journal of Visualized Experiments, 2019, , .	0.3	0
46	[¹⁸ F]‣odium Fluoride PET/MR Imaging for Bone–Cartilage Interactions in Hip Osteoarthritis: A Feasibility Study. Journal of Orthopaedic Research, 2019, 37, 2671-2680.	2.3	17
47	Hip joint muscle forces during gait in patients with femoroacetabular impingement syndrome are associated with patient reported outcomes and cartilage composition. Journal of Biomechanics, 2019, 84, 138-146.	2.1	22
48	Applying Densely Connected Convolutional Neural Networks for Staging Osteoarthritis Severity from Plain Radiographs. Journal of Digital Imaging, 2019, 32, 471-477.	2.9	106
49	3D convolutional neural networks for detection and severity staging of meniscus and PFJ cartilage morphological degenerative changes in osteoarthritis and anterior cruciate ligament subjects. Journal of Magnetic Resonance Imaging, 2019, 49, 400-410.	3.4	98
50	MR study of longitudinal variations in proximal femur 3D morphological shape and associations with cartilage health in hip osteoarthritis. Journal of Orthopaedic Research, 2019, 37, 161-170.	2.3	12
51	Translation of morphological and functional musculoskeletal imaging. Journal of Orthopaedic Research, 2019, 37, 23-34.	2.3	9
52	Study of the interactions between proximal femur 3d bone shape, cartilage health, and biomechanics in patients with hip Osteoarthritis. Journal of Orthopaedic Research, 2018, 36, 330-341.	2.3	24
53	A novel mrâ€based method for detection of cartilage delamination in femoroacetabular impingement patients. Journal of Orthopaedic Research, 2018, 36, 971-978.	2.3	15
54	Femoroacetabular impingement and hip OsteoaRthritis Cohort (FORCe): protocol for a prospective study. Journal of Physiotherapy, 2018, 64, 55.	1.7	27

#	Article	IF	CITATIONS
55	Local associations between knee cartilage T 1ï•and T 2 relaxation times and patellofemoral joint stress during walking: A voxel-based relaxometry analysis. Knee, 2018, 25, 406-416.	1.6	12
56	Use of 2D U-Net Convolutional Neural Networks for Automated Cartilage and Meniscus Segmentation of Knee MR Imaging Data to Determine Relaxometry and Morphometry. Radiology, 2018, 288, 177-185.	7.3	291
57	MRI and biomechanics multidimensional data analysis reveals R ₂ â€R _{1Ï} as an early predictor of cartilage lesion progression in knee osteoarthritis. Journal of Magnetic Resonance Imaging, 2018, 47, 78-90.	3.4	40
58	Sagittal plane walking patterns are related to MRI changes over 18â€months in people with and without mildâ€moderate hip osteoarthritis. Journal of Orthopaedic Research, 2018, 36, 1472-1477.	2.3	19
59	Using the Scoring Hip Osteoarthritis with Magnetic Resonance Imaging (SHOMRI) system to assess intraâ€articular pathology in femoroacetabular impingement. Journal of Orthopaedic Research, 2018, 36, 3064-3070.	2.3	7
60	High-Resolution Imaging Techniques for Bone Quality Assessment. , 2018, , 1007-1041.		3
61	Using multidimensional topological data analysis to identify traits of hip osteoarthritis. Journal of Magnetic Resonance Imaging, 2018, 48, 1046-1058.	3.4	12
62	Accelerated Bone Loss in Older Men: Effects on Bone Microarchitecture and Strength. Journal of Bone and Mineral Research, 2018, 33, 1859-1869.	2.8	12
63	Correlation of Patient Symptoms With Labral and Articular Cartilage Damage in Femoroacetabular Impingement. Orthopaedic Journal of Sports Medicine, 2018, 6, 232596711877878.	1.7	21
64	Baseline cartilage quality is associated with voxelâ€based <i>T</i> _{1Ï} and <i>T</i> ₂ following ACL reconstruction: A multicenter pilot study. Journal of Orthopaedic Research, 2017, 35, 688-698.	2.3	28
65	Longitudinal study using voxel-based relaxometry: Association between cartilage T1ϕand T2 and patient reported outcome changes in hip osteoarthritis. Journal of Magnetic Resonance Imaging, 2017, 45, 1523-1533.	3.4	35
66	Positive contrast from cells labeled with iron oxide nanoparticles: Quantitation of imaging data. Magnetic Resonance in Medicine, 2017, 78, 1900-1910.	3.0	12
67	Joint Loading in the Sagittal Plane During Gait Is Associated With Hip Joint Abnormalities in Patients With Femoroacetabular Impingement. American Journal of Sports Medicine, 2017, 45, 810-818.	4.2	37
68	Effects of Surgical Factors on Cartilage Can Be Detected Using Quantitative Magnetic Resonance Imaging After Anterior Cruciate Ligament Reconstruction. American Journal of Sports Medicine, 2017, 45, 1075-1084.	4.2	16
69	Cyclops lesions detected by MRI are frequent findings after ACL surgical reconstruction but do not impact clinical outcome over 2Âyears. European Radiology, 2017, 27, 3499-3508.	4.5	25
70	[¹⁸ F]-Sodium Fluoride PET MR–Based Localization and Quantification of Bone Turnover as a Biomarker for Facet Joint–Induced Disability. American Journal of Neuroradiology, 2017, 38, 2028-2031.	2.4	13
71	Statistical Parametric Mapping of HR-pQCT Images: A Tool for Population-Based Local Comparisons of Micro-Scale Bone Features. Annals of Biomedical Engineering, 2017, 45, 949-962.	2.5	9
72	Evolution of Intrameniscal Signal-Intensity Alterations Detected on MRI Over 24 Months in Patients With Traumatic Anterior Cruciate Ligament Tear. American Journal of Roentgenology, 2017, 208, 386-392.	2.2	4

#	Article	IF	CITATIONS
73	Composite metric <i>R</i> ₂ â^ <i>R</i> _{1Ï} (1/ <i>T</i> ₂ â^ 1/ <i>T</i> _{1Ï}) as a potential MR imaging biomarker associated changes in pain after ACL reconstruction: A sixâ€month followâ€up. Journal of Orthopaedic Research, 2017, 35, 718-729.	l with 2.3	17
74	Abnormal Joint Moment Distributions and Functional Performance During Sitâ€ŧo tand in Femoroacetabular Impingement Patients. PM and R, 2017, 9, 563-570.	1.6	18
75	iPhone Sensors in Tracking Outcome Variables of the 30-Second Chair Stand Test and Stair Climb Test to Evaluate Disability: Cross-Sectional Pilot Study. JMIR MHealth and UHealth, 2017, 5, e166.	3.7	17
76	Principal component analysis-T1ϕvoxel based relaxometry of the articular cartilage: a comparison of biochemical patterns in osteoarthritis and anterior cruciate ligament subjects. Quantitative Imaging in Medicine and Surgery, 2016, 6, 623-633.	2.0	13
77	Fully automatic analysis of the knee articular cartilageT1ïrelaxation time using voxel-based relaxometry. Journal of Magnetic Resonance Imaging, 2016, 43, 970-980.	3.4	80
78	Microarchitecture and Peripheral BMD are Impaired in Postmenopausal White Women With Fracture Independently of Total Hip <i>T</i> -Score: An International Multicenter Study. Journal of Bone and Mineral Research, 2016, 31, 1158-1166.	2.8	69
79	Kartogenin treatment prevented joint degeneration in a rodent model of osteoarthritis: A pilot study. Journal of Orthopaedic Research, 2016, 34, 1780-1789.	2.3	37
80	Bone microstructure in men assessed by HR-pQCT: Associations with risk factors and differences between men with normal, low, and osteoporosis-range areal BMD. Bone Reports, 2016, 5, 312-319.	0.4	7
81	Longitudinal assessment of MRI in hip osteoarthritis using SHOMRI and correlation with clinical progression. Seminars in Arthritis and Rheumatism, 2016, 45, 648-655.	3.4	26
82	lmaging Bone–Cartilage Interactions in Osteoarthritis Using [¹⁸ F]-NaF PET-MRI. Molecular Imaging, 2016, 15, 153601211668359.	1.4	50
83	Quantitative magnetic resonance arthrography in patients with femoroacetabular impingement. Journal of Magnetic Resonance Imaging, 2016, 44, 1539-1545.	3.4	10
84	Zonal differences in meniscus MR relaxation times in response to in vivo static loading in knee osteoarthritis. Journal of Orthopaedic Research, 2016, 34, 249-261.	2.3	19
85	<i>T</i> _{1ï} and <i>T</i> ₂ â€based characterization of regional variations in intervertebral discs to detect early degenerative changes. Journal of Orthopaedic Research, 2016, 34, 1373-1381.	2.3	36
86	Loaded versus unloaded magnetic resonance imaging (MRI) of the knee: Effect on meniscus extrusion in healthy volunteers and patients with osteoarthritis. European Journal of Radiology Open, 2016, 3, 100-107.	1.6	51
87	Quantification of bone marrow water and lipid composition in anterior cruciate ligament-injured and osteoarthritic knees using three-dimensional magnetic resonance spectroscopic imaging. Magnetic Resonance Imaging, 2016, 34, 632-637.	1.8	17
88	Segmentation of joint and musculoskeletal tissue in the study of arthritis. Magnetic Resonance Materials in Physics, Biology, and Medicine, 2016, 29, 207-221.	2.0	59
89	18F-sodium fluoride PET-CT hybrid imaging of the lumbar facet joints: Tracer uptake and degree of correlation to CT-graded arthropathy. World Journal of Nuclear Medicine, 2016, 15, 85-90.	0.5	20
90	Scoring hip osteoarthritis with MRI (SHOMRI): A whole joint osteoarthritis evaluation system. Journal of Magnetic Resonance Imaging, 2015, 41, 1549-1557.	3.4	98

#	Article	IF	CITATIONS
91	Improved differentiation between knees with cartilage lesions and controls using 7T relaxation time mapping. Journal of Orthopaedic Translation, 2015, 3, 197-204.	3.9	21
92	Acetabular cartilage defects cause altered hip and knee joint coordination variability during gait. Clinical Biomechanics, 2015, 30, 1202-1209.	1.2	18
93	Anatomic correlates of reduced hip extension during walking in individuals with mildâ€moderate radiographic hip osteoarthritis. Journal of Orthopaedic Research, 2015, 33, 527-534.	2.3	39
94	Individuals with isolated patellofemoral joint osteoarthritis exhibit higher mechanical loading at the knee during the second half of the stance phase. Clinical Biomechanics, 2015, 30, 383-390.	1.2	30
95	Spatial distribution of intracortical porosity varies across age and sex. Bone, 2015, 75, 88-95.	2.9	38
96	Higher Knee Flexion Moment During the Second Half of the Stance Phase of Gait Is Associated With the Progression of Osteoarthritis of the Patellofemoral Joint on Magnetic Resonance Imaging. Journal of Orthopaedic and Sports Physical Therapy, 2015, 45, 656-664.	3.5	50
97	Simultaneous acquisition of T _{1Ï} and T ₂ quantification in knee cartilage: Repeatability and diurnal variation. Journal of Magnetic Resonance Imaging, 2014, 39, 1287-1293.	3.4	105
98	Improving bone strength prediction in human proximal femur specimens through geometrical characterization of trabecular bone microarchitecture and support vector regression. Journal of Electronic Imaging, 2014, 23, 013013.	0.9	28
99	Comparison of T1rho relaxation times between ACL-reconstructed knees and contralateral uninjured knees. Knee Surgery, Sports Traumatology, Arthroscopy, 2014, 22, 298-307.	4.2	70
100	Differences in the Association of Hip Cartilage Lesions and Camâ€Type Femoroacetabular Impingement With Movement Patterns: A Preliminary Study. PM and R, 2014, 6, 681-689.	1.6	56
101	Three-dimensional analysis of subchondral cysts in hip osteoarthritis: An ex vivo HR-pQCT study. Bone, 2014, 66, 140-145.	2.9	28
102	Quantitative In Vivo HR-pQCT Imaging of 3D Wrist and Metacarpophalangeal Joint Space Width in Rheumatoid Arthritis. Annals of Biomedical Engineering, 2013, 41, 2553-2564.	2.5	60
103	Quantitative MRI of articular cartilage and its clinical applications. Journal of Magnetic Resonance Imaging, 2013, 38, 991-1008.	3.4	98
104	Regional variations in MR relaxation of hip joint cartilage in subjects with and without femoralacetabular impingement. Magnetic Resonance Imaging, 2013, 31, 1129-1136.	1.8	50
105	T1rho MRI relaxation in knee OA subjects with varying sizes of cartilage lesions. Knee, 2013, 20, 113-119.	1.6	44
106	Age- and gender-related differences in cortical geometry and microstructure: Improved sensitivity by regional analysis. Bone, 2013, 52, 623-631.	2.9	51
107	Predicting the biomechanical strength of proximal femur specimens through high dimensional geometric features and support vector regression. , 2013, 8672, .		0
108	Multicenter precision of cortical and trabecular bone quality measures assessed by high-resolution peripheral quantitative computed tomography. Journal of Bone and Mineral Research, 2013, 28, 524-536.	2.8	98

#	Article	IF	CITATIONS
109	Quantitative MRI of articular cartilage and its clinical applications. Journal of Magnetic Resonance Imaging, 2013, 38, spcone-spcone.	3.4	0
110	In Vivo Intervertebral Disc Characterization Using Magnetic Resonance Spectroscopy and T1ϕImaging. Spine, 2012, 37, 214-221.	2.0	58
111	The effect of voxel size on highâ€resolution peripheral computed tomography measurements of trabecular and cortical bone microstructure. Medical Physics, 2012, 39, 1893-1903.	3.0	96
112	The Acute Effect of Running on Knee Articular Cartilage and Meniscus Magnetic Resonance Relaxation Times in Young Healthy Adults. American Journal of Sports Medicine, 2012, 40, 2134-2141.	4.2	94
113	Diagnostic Tools and Imaging Methods in Intervertebral Disk Degeneration. Orthopedic Clinics of North America, 2011, 42, 501-511.	1.2	21
114	Quantitative characterization of subject motion in HR-pQCT images of the distal radius and tibia. Bone, 2011, 48, 1291-1297.	2.9	88
115	Longitudinal analysis of MRI <i>T</i> ₂ knee cartilage laminar organization in a subset of patients from the osteoarthritis initiative: A texture approach. Magnetic Resonance in Medicine, 2011, 65, 1184-1194.	3.0	51
116	Atlasâ€based knee cartilage assessment. Magnetic Resonance in Medicine, 2011, 66, 575-581.	3.0	26
117	Micrometer-sized iron oxide particle labeling of mesenchymal stem cells for magnetic resonance imaging-based monitoring of cartilage tissue engineering. Magnetic Resonance Imaging, 2011, 29, 40-49.	1.8	39
118	Quantitative MRI using T1ϕand T2 in human osteoarthritic cartilage specimens: correlation with biochemical measurements and histology. Magnetic Resonance Imaging, 2011, 29, 324-334.	1.8	206
119	Cartilage in Anterior Cruciate Ligament–Reconstructed Knees: MR Imaging T1 _Ï and T2—Initial Experience with 1-year Follow-up. Radiology, 2011, 258, 505-514.	7.3	192
120	Age- and gender-related differences in the geometric properties and biomechanical significance of intracortical porosity in the distal radius and tibia. Journal of Bone and Mineral Research, 2010, 25, 983-993.	2.8	271
121	A longitudinal HR-pQCT study of alendronate treatment in postmenopausal women with low bone density: Relations among density, cortical and trabecular microarchitecture, biomechanics, and bone turnover. Journal of Bone and Mineral Research, 2010, 25, 2558-2571.	2.8	210
122	T _{1Ï} and T ₂ quantitative magnetic resonance imaging analysis of cartilage regeneration following microfracture and mosaicplasty cartilage resurfacing procedures. Journal of Magnetic Resonance Imaging, 2010, 32, 914-923.	3.4	39
123	In vivo 3.0â€ŧesla magnetic resonance <i>T</i> _{1Ï} and <i>T</i> ₂ relaxation mapping in subjects with intervertebral disc degeneration and clinical symptoms. Magnetic Resonance in Medicine, 2010, 63, 1193-1200.	3.0	116
124	Regional variations of gender-specific and age-related differences in trabecular bone structure of the distal radius and tibia. Bone, 2010, 46, 1652-1660.	2.9	66
125	Reproducibility of direct quantitative measures of cortical bone microarchitecture of the distal radius and tibia by HR-pQCT. Bone, 2010, 47, 519-528.	2.9	397
126	Spatial analysis of magnetic resonance and relaxation times improves classification between subjects with and without osteoarthritis. Medical Physics, 2009, 36, 4059-4067.	3.0	71

#	Article	IF	CITATIONS
127	Spatial distribution and relationship of <i>T</i> _{1Ï} and <i>T</i> ₂ relaxation times in knee cartilage with osteoarthritis. Magnetic Resonance in Medicine, 2009, 61, 1310-1318.	3.0	129
128	Assessment of intervertebral disc degeneration with magnetic resonance singleâ€voxel spectroscopy. Magnetic Resonance in Medicine, 2009, 62, 1140-1146.	3.0	34
129	T1rho, T2 and focal knee cartilage abnormalities in physically active and sedentary healthy subjects versus early OA patients—a 3.0-Tesla MRI study. European Radiology, 2009, 19, 132-143.	4.5	195
130	Magnetic Resonance Imaging of 3-Dimensional In Vivo Tibiofemoral Kinematics in Anterior Cruciate Ligament–Reconstructed Knees. Arthroscopy - Journal of Arthroscopic and Related Surgery, 2009, 25, 760-766.	2.7	62
131	In Vivo Determination of Bone Structure in Postmenopausal Women: A Comparison of HR-pQCT and High-Field MR Imaging. Journal of Bone and Mineral Research, 2008, 23, 463-474.	2.8	122
132	Magnetic resonance imaging for osteoporosis. Skeletal Radiology, 2008, 37, 95-97.	2.0	30
133	Quantitative assessment of bone marrow edemaâ€like lesion and overlying cartilage in knees with osteoarthritis and anterior cruciate ligament tear using MR imaging and spectroscopic imaging at 3 Tesla. Journal of Magnetic Resonance Imaging, 2008, 28, 453-461.	3.4	93
134	In vivo <i>T</i> _{1ï} mapping in cartilage using 3D magnetizationâ€prepared angleâ€modulated partitioned <i>k</i> â€space spoiled gradient echo snapshots (3D MAPSS). Magnetic Resonance in Medicine, 2008, 59, 298-307.	3.0	163
135	New techniques for cartilage magnetic resonance imaging relaxation time analysis: Texture analysis of flattened cartilage and localized intra―and interâ€subject comparisons. Magnetic Resonance in Medicine, 2008, 59, 1472-1477.	3.0	52
136	Inter-subject comparison of MRI knee cartilage thickness. Medical Image Analysis, 2008, 12, 120-135.	11.6	127
137	A comparative study at 3 T of sequence dependence of T2 quantitation in the knee. Magnetic Resonance Imaging, 2008, 26, 1215-1220.	1.8	94
138	Relationship between trabecular bone structure and articular cartilage morphology and relaxation times in early OA of the knee joint using parallel MRI at 3T. Osteoarthritis and Cartilage, 2008, 16, 1150-1159.	1.3	119
139	Lactic Acid and Proteoglycans as Metabolic Markers for Discogenic Back Pain. Spine, 2008, 33, 312-317.	2.0	60
140	In Vivo T1ϕQuantitative Assessment of Knee Cartilage After Anterior Cruciate Ligament Injury Using 3 Tesla Magnetic Resonance Imaging. Investigative Radiology, 2008, 43, 782-788.	6.2	59
141	An eight-channel, nonoverlapping phased array coil with capacitive decoupling for parallel MRI at 3 T. Concepts in Magnetic Resonance Part B, 2007, 31B, 37-43.	0.7	40
142	In vivo bone and cartilage MRI using fullyâ€balanced steadyâ€state freeâ€precession at 7 tesla. Magnetic Resonance in Medicine, 2007, 58, 1294-1298.	3.0	59
143	A Local Adaptive Threshold Strategy for High Resolution Peripheral Quantitative Computed Tomography of Trabecular Bone. Annals of Biomedical Engineering, 2007, 35, 1678-1686.	2.5	104
144	A feasibility study of in vivo T1ϕimaging of the intervertebral disc. Magnetic Resonance Imaging, 2006, 24, 1001-1007.	1.8	47

#	Article	IF	CITATIONS
145	Correlation of HR-MAS Spectroscopy Derived Metabolite Concentrations With Collagen and Proteoglycan Levels and Thompson Grade in the Degenerative Disc. Spine, 2005, 30, 2683-2688.	2.0	31
146	Characterization of intervertebral disc degeneration by high-resolution magic angle spinning (HR-MAS) spectroscopy. Magnetic Resonance in Medicine, 2005, 53, 519-527.	3.0	44
147	In vivo 3T spiral imaging based multi-slice T1ϕmapping of knee cartilage in osteoarthritis. Magnetic Resonance in Medicine, 2005, 54, 929-936.	3.0	158
148	Hyaluronan Increases RANKL Expression in Bone Marrow Stromal Cells Through CD44. Journal of Bone and Mineral Research, 2005, 20, 30-40.	2.8	7
149	T2 Relaxation Time of Cartilage at MR Imaging: Comparison with Severity of Knee Osteoarthritis. Radiology, 2004, 232, 592-598.	7.3	475
150	A pilot, two-year longitudinal study of the interrelationship between trabecular bone and articular cartilage in the osteoarthritic knee. Osteoarthritis and Cartilage, 2004, 12, 997-1005.	1.3	109
151	Diffraction enhanced imaging of articular cartilage and comparison with micro-computed tomography of the underlying bone structure. European Radiology, 2004, 14, 1440-8.	4.5	33
152	T2 relaxation time measurements in osteoarthritis. Magnetic Resonance Imaging, 2004, 22, 673-682.	1.8	212
153	Current technologies in the evaluation of bone architecture. Current Osteoporosis Reports, 2003, 1, 105-109.	3.6	9
154	Osteoarthritis: MR Imaging Findings in Different Stages of Disease and Correlation with Clinical Findings. Radiology, 2003, 226, 373-381.	7.3	444
155	Current technologies in the evaluation of bone architecture. Current Osteoporosis Reports, 2003, 1, 105-109.	3.6	0
156	Magnetic Resonance Imaging of Trabecular Bone Structure. Topics in Magnetic Resonance Imaging, 2002, 13, 323-334.	1.2	101
157	Magnetic Resonance Imaging Measurement of Relaxation and Water Diffusion in the Human Lumbar Intervertebral Disc Under Compression In Vitro. Spine, 2001, 26, E437-E444.	2.0	113
158	The Skeletal Structure of Insulin-Like Growth Factor I-Deficient Mice. Journal of Bone and Mineral Research, 2001, 16, 2320-2329.	2.8	175
159	Trabecular Structure Assessment in Lumbar Vertebrae Specimens Using Quantitative Magnetic Resonance Imaging and Relationship with Mechanical Competence. Journal of Bone and Mineral Research, 2001, 16, 1511-1519.	2.8	35
160	In vivoassessment of trabecular bone structure using fractal analysis of distal radius radiographs. Medical Physics, 2000, 27, 2594-2599.	3.0	42
161	Fractal analysis of radiographs: Assessment of trabecular bone structure and prediction of elastic modulus and strength. Medical Physics, 1999, 26, 1330-1340.	3.0	97
162	A Comparative Study of Trabecular Bone Properties in the Spine and Femur Using High Resolution MRI and CT. Journal of Bone and Mineral Research, 1998, 13, 122-132.	2.8	159

#	Article	IF	CITATIONS
163	Trabecular Bone Mineral and Calculated Structure of Human Bone Specimens Scanned by Peripheral Quantitative Computed Tomography: Relation to Biomechanical Properties. Journal of Bone and Mineral Research, 1998, 13, 1783-1790.	2.8	90
164	In Vivo High Resolution MRI of the Calcaneus: Differences in Trabecular Structure in Osteoporosis Patients. Journal of Bone and Mineral Research, 1998, 13, 1175-1182.	2.8	261
165	Morphometric texture analysis of spinal trabecular bone structure assessed using orthogonal radiographic projections. Medical Physics, 1998, 25, 2037-2045.	3.0	41
166	Fractal Based Image Analysis of Human Trabecular Bone using the Box Counting Algorithm. Fractals, 1998, 06, 275-283.	3.7	12
167	Decay characteristics of bone marrow in the presence of a trabecular bone network:In vitro andin vivo studies showing a departure from monoexponential behavior. Magnetic Resonance in Medicine, 1996, 35, 921-927.	3.0	19
168	Quantitative MR relaxometry study of muscle composition and function in duchenne muscular dystrophy. Journal of Magnetic Resonance Imaging, 1994, 4, 59-64.	3.4	94
169	Fractal geometry and vertebral compression fractures. Journal of Bone and Mineral Research, 1994, 9, 1797-1802.	2.8	83
170	Application of fractal geometry techniques to the study of trabecular bone. Medical Physics, 1993, 20, 1611-1619.	3.0	118
171	In vivo relationship between marrow T2* and trabecular bone density determined with a chemical shift—selective asymmetric spin-echo sequence. Journal of Magnetic Resonance Imaging, 1992, 2, 209-219	3.4	104